

PromptLA: Towards Integrity Verification of Black-box Text-to-Image Diffusion Models

Zhuomeng Zhang
zzmsmm@sjtu.edu.cn
Shanghai Jiao Tong University
Shanghai, China

Chong Di
cdi@qju.edu.cn
Qilu University of Technology
Jinan, China

Fangqi Li
solour_lfq@sjtu.edu.cn
Shanghai Jiao Tong University
Shanghai, China

Shilin Wang
wsl@sjtu.edu.cn
Shanghai Jiao Tong University
Shanghai, China

Abstract

Current text-to-image (T2I) diffusion models can produce high-quality images, and malicious users who are authorized to use the model only for benign purposes might modify their models to generate images that result in harmful social impacts. Therefore, it is essential to verify the integrity of T2I diffusion models, especially when they are deployed as black-box services. To this end, considering the randomness within the outputs of generative models and the high costs in interacting with them, we capture modifications to the model through the differences in the distributions of the features of generated images. We propose a novel prompt selection algorithm based on learning automaton for efficient and accurate integrity verification of T2I diffusion models. Extensive experiments demonstrate the effectiveness, stability, accuracy and generalization of our algorithm against existing integrity violations compared with baselines. To the best of our knowledge, this paper is the first work addressing the integrity verification of T2I diffusion models, which paves the way to copyright discussions and protections for artificial intelligence applications in practice.

1 Introduction

Generative artificial intelligence has made significant progress in recent years. Notably, text-to-image (T2I) models [9, 22–24, 28], exemplified by Stable Diffusion (SD) [25], have found widespread applications. To generate unique and stylized images, methods including Textual Inversion [12], DreamBooth [26] and LoRA [27] have been proposed as convenient tuning schemes for T2I diffusion models. However, malicious users can also take advantage of these techniques to breach the integrity of models and produce misleading and illegal images, even when they are not authorized to do so. Therefore, in the commercial scenario where the model is only authorized for using as it is, it is essential to verify the integrity of T2I diffusion models to ensure that users do not modify the model through any technique. Upon the occurrence of misconducts, an integrity verification method should attribute malicious behaviors to the user rather than the model’s original owner, as shown in Figure 1.

However, research on the integrity of T2I diffusion models is relatively lacking, with most work focusing on ownership verification, such as Stable Signature [11] and Tree-ring [33]. In the field

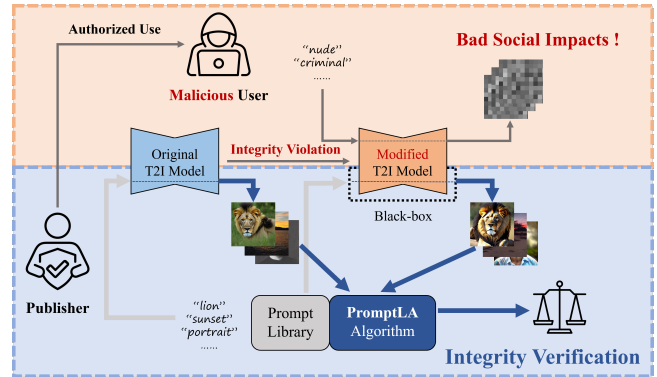


Figure 1: The proposed integrity verification framework of T2I diffusion models. PromptLA selects prompts for optimal efficiency.

of integrity verification, the focus has remained on relatively basic classification tasks.

Compared with the integrity verification of models for classification tasks, integrity verification of T2I diffusion models has the following characteristics: (i) **randomness**, (ii) **complexity**, and (iii) **high access costs**, as shown in Table 1. The integrity of classifiers can be examined by whether their predictions change for some trigger samples or not. However, due to the stochastic nature of the diffusion process, it is impossible to determine the integrity of models by simply comparing generated images for a fixed prompt. Moreover, generated images are inherently more complex compared to labels, and accessing the generated images of the model requires more time, which increases the difficulty of integrity verification. Reflecting modifications to models through generated images and selecting prompts for efficient integrity verification are key challenges in achieving integrity verification of T2I diffusion models.

To address the aforementioned challenges in verifying the integrity of T2I diffusion models, this paper makes the following contributions:

- To the best of our knowledge, this paper is the first integrity verification scheme for T2I diffusion models. The difference

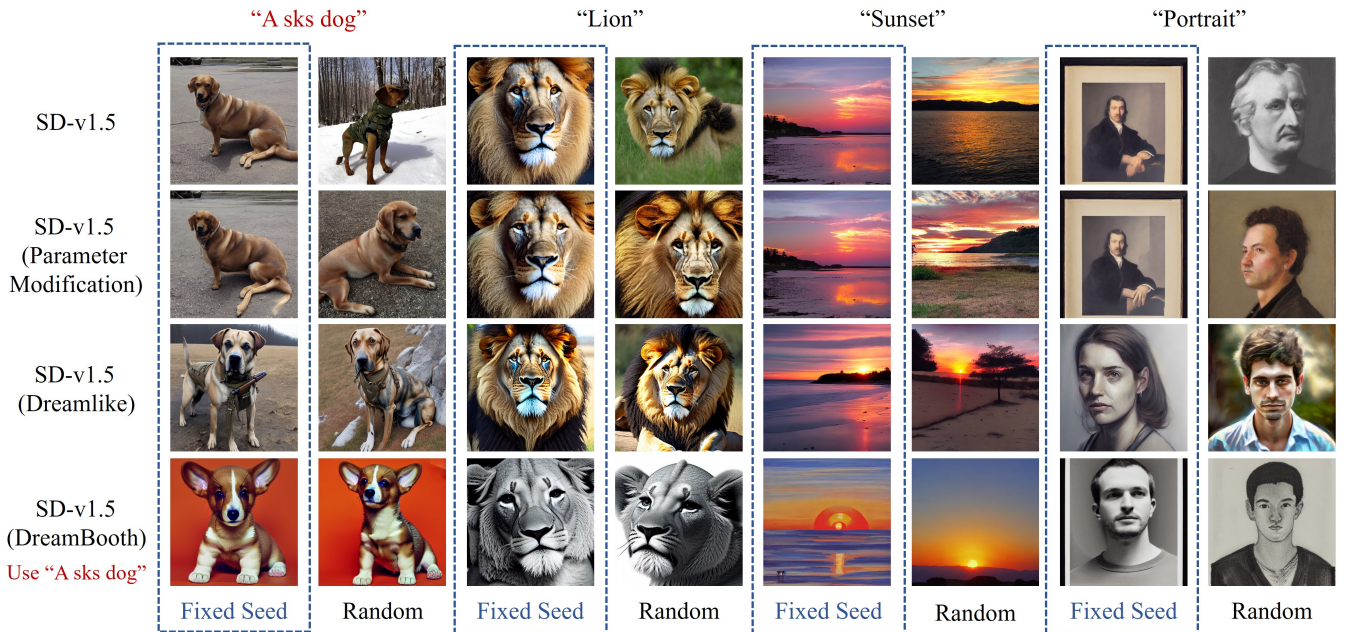


Figure 2: Comparison of images generated by the original model and after various integrity violations. For each prompt, the left column shows images generated with a fixed seed, and the right column shows randomly generated images. The details of integrity violations refer to the experiment section.

between models is measured in the differences in the distributions of feature of their generated images.

- We explore the impact of prompts on the feature distribution differences in generated images, and propose a prompt selection algorithm based on learning automaton to achieve precise and efficient integrity verification.
- Extensive experimental results indicate that our algorithm exhibits a high detection accuracy and efficiency against various integrity violations, and remains stable against image-level post-processing.

2 Preliminary

2.1 Threat Model

During the integrity verification, a malicious user obtains the original model f_0 and modifies it using some strategy m , resulting in a modified model f_m . In the white-box scenario, integrity violations are detected by comparing the hash values of weights [39] of f_0 and f_m , after eliminating the structural symmetries [19]:

$$\text{hash}(f_m) \neq \text{hash}(f_0) \Rightarrow f_m \neq f_0. \quad (1)$$

In the black-box scenario, the internal weights cannot be accessed so the hash of a model is intractable. Instead, two models are judged to be different only if their performance can be differentiated. This paper focuses on the black-box scenario.

Typical integrity violations of models for classification tasks include pruning [34], fine-tuning [4], feature extraction [37], etc. The integrity verification of classifiers uniformly relies on their outputs on a series of triggers $T = \{t_n\}_{n=1}^N$, which constitute their fragile fingerprints. If f_m disagrees with f_0 on at least one trigger

Table 1: Characteristics of T2I diffusion models compared to classification tasks.

Task	Randomness of outputs	Complexity of outputs	Query cost
Classification	Deterministic	Simple	Low
Text-to-Image	Random	Complex	High

then the integrity violation is detected:

$$\exists t_n \in T, f_m(t_n) \neq f_0(t_n) \Rightarrow f_m \neq f_0. \quad (2)$$

The triggers T should be samples sensitive to model changes [15, 35], e.g., samples close to the decision boundary [2, 32, 38].

2.1.1 Integrity verification of T2I diffusion models End-to-end fine-tuning becomes difficult for large T2I diffusion models. Instead, the toolkit for modifying T2I diffusion models includes DreamBooth [26], LoRA [27], direct parameter modifications, etc, which can also be used to breach the integrity of models. Integrity verification of T2I diffusion models is tantamount to find a prompt \mathbf{p} such that $f_m(\mathbf{p})$ can be distinguished from $f_0(\mathbf{p})$. As shown in Figure 2, on the prompt which was used to conduct an integrity violation ("A sks dog" here), generated images from f_m and f_0 can be easily distinguished. After eliminating the randomness by fixing the generator seed, a trivial comparison between images generated by different T2I diffusion models yields assertions on the integrity. However, the defender cannot always know the prompts used to conduct integrity violations, and the same model might produce different images given the same prompt due to the randomness in

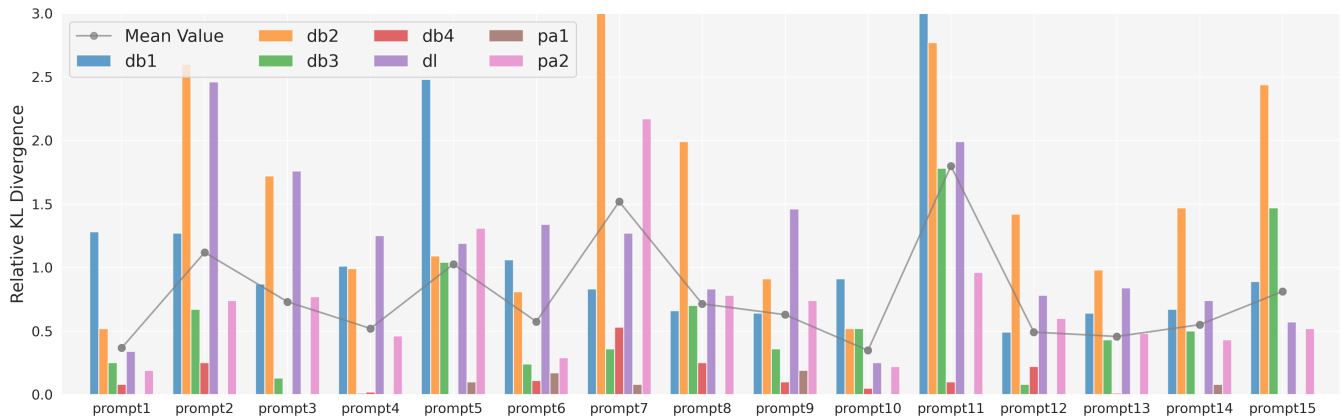


Figure 3: The relative KL divergence differences in the distribution of features extracted from images generated by T2I diffusion models before and after various integrity violations, using different prompt. The size of prompt library is set to 50 (15 of them are shown here), which is generated by GPT-4. Different colors represent different integrity violations, 'db1-4' represents DreamBooth, 'dl' represents Fine-tuning and 'pa1-2' represents Parameter Modification. The details of integrity violations refer to the experiment section. The distribution of generated images' features is estimated using 50 images each.

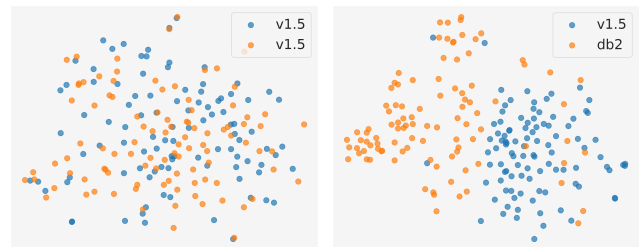
diffusion process. Meanwhile, querying T2I models is usually more expensive than querying classifiers.

Considering the characteristics of T2I diffusion models compared to classification tasks, as shown in Table 1, the integrity verification of T2I diffusion models should: (I) Measure the modifications to the underlying T2I diffusion models from the randomly generated images. (II) Cut down on the number of queries while ensuring the integrity violation can be detected with a high accuracy.

2.2 Related Work

2.2.1 Detection and tracing of AI-generated images Most existing studies focus on detection and tracing of a generated image using color-based [20], frequency-based [10], or learning-based [36] features. ManiFPT [30] applies these methods to the tracing of generated images from various models, including GANs [14], VAE, and LDM [25], etc. The intuition behind these copyright tracing methods is to extract the evidence embedded in the generated images during the generation process that characterizes the generative model. The same intuition also motivates our work: it is possible to extract fine-grained information from generated images that reflects the characteristics of the generative model, thereby telling whether the model has been tampered with or not.

2.2.2 Learning automaton As a fundamental component of non-associative reinforcement learning, wherein the environment operates independently of the input actions, Learning Automaton (LA) seeks to evaluate the efficacy of actions in an unknown environment through iterative interactions, ultimately identifying the optimal action among available choices [21]. Owing to its adaptive capabilities, LA has been extensively employed in various applications, including mathematical optimization [7], pattern recognition [29], cybersecurity [3], and data mining [5].



(a) v1.5-v1.5

(b) v1.5-DreamBooth

Figure 4: tSNE of features extracted from generated images using the Inception-v3 model and prompt7 "abstract". (a) Comparison within the original model SD-v1.5. (b) Comparison between the original model and the model fine-tuned using DreamBooth.

3 Method

3.1 Model Differences Measurement

To address the random nature of outputs from text-to-image (T2I) models, we follow the motivation that modifications to the model can be reflected in the feature distribution of generated images. This motivation is verified by an example shown in Figure 4, where the feature distribution of images generated by models fine-tuned using the DreamBooth differs from the feature distribution of images generated by the original model with the same prompt.

To numerically measure the distance between randomly generated images from T2I diffusion models under the same prompt, we leverage the KL divergence [16] and employ a variational approach by assuming that the underlying distributions of features is a multivariate normal distribution [13, 17, 18] and further reduce the bias with standard Bayesian estimation with non-informative prior [40].

Formally, for the fixed prompt \mathbf{p} and T2I diffusion model f , we extract a collection of features $t_{\mathbf{p}}(f)$ by querying f for n times:

$$t_{\mathbf{p}}(f) = \{\mathcal{E}(\tau_l) | \tau_l \leftarrow f(\mathbf{p})\}_{l=1}^n. \quad (3)$$

where \mathcal{E} is a feature extractor. Inception-v3 [31] pre-trained on ImageNet [6] is used as \mathcal{E} . Given the original model f_0 and the suspicious model f_m , their outputs on a prompt \mathbf{p} are featured by $t_{\mathbf{p}}(f_0)$, $t_{\mathbf{p}}(f_m)$, which are then approximated by two multivariate normal distributions $P(t_{\mathbf{p}}(f_0)) \sim \mathcal{N}(\mu_P, \Sigma_P)$ and $Q(t_{\mathbf{p}}(f_m)) \sim \mathcal{N}(\mu_Q, \Sigma_Q)$ respectively. So the distance between two distributions can be computed by:

$$D_{KL}(P||Q) = \int P(X) \log \frac{P(X)}{Q(X)} dX. \quad (4)$$

To better compare different prompts, we use relative KL divergence to mitigate the impact of internal randomness on the KL divergence:

$$\beta_{\mathbf{p}} = \frac{D_{KL}(P||Q)}{D_{KL}(P||P')} - 1. \quad (5)$$

where P' is another independent estimation on the distribution of $t_{\mathbf{p}}(f_0)$.

As shown in Figure 3, the distance between distributions of features of images generated by the model before and after integrity violations varies significantly with the prompt. Therefore, the integrity verification depends on maximizing the distance between distributions of features corresponding to certain prompts, which can be further reduced to selecting discriminating prompts.

Table 2: Notations used in PromptLA algorithm.

Symbol	Explanation
α	Significance level.
r	The number of round, $r \in \{1, 2, \dots, R\}$.
R_s	The number of round to start the hypothesis test.
R_e	The total number of rounds.
$A(r)$	Action set at the r -th round.
q	Size of A , $ A(1) = A = q$.
$\beta_i^r(k)$	Feedback for k -th choose for action a_i at the r -th round.
$F_i(r)$	Feedback sequence for action a_i at the r -th round.
n	The number of images generated per prompt per round.
$\hat{d}_i(r)$	Mean of the feedback sequence $F_i(r)$.
$a_{m(r)}$	Estimated optimal action after the r -th round.

3.2 PromptLA

We remark that selecting the most discriminating prompt from a pool of candidates by interacting with black-box T2I diffusion models with the least number of queries is essentially a stochastic optimization task, which can be efficiently solved by reinforcement learning algorithms. We combine the learning automaton (LA) framework based on statistical hypothesis testing approach [8] and design a prompt selection algorithm (PromptLA). In a nutshell, an LA interacts with a stochastic environment (i.e., the feedback from the environment might be different even when the LA chooses the same action) by continually selecting actions, updating its strategy, and converging to the optimal action. In our setting, the environment consists of two T2I diffusion models $\{f_0, f_m\}$, while the set of actions is the set of candidate prompts. The notations that are used in defining the algorithm are summarized in Table 2.

Algorithm 1 PromptLA

Input: A, f_0, f_m .

Parameter: α, R_s, R_e, n .

Output: a_m, \hat{d}_m .

```

1: Let  $r = 1, A(1) = A, \forall a_i \in A, F_i(0) = \emptyset$ .
2: while  $r \leq R_e$  and  $|A(r)| > 1$  do
3:   for  $a_i \in A(r)$  do
4:      $F_i(r) = F_i(r-1)$ 
5:     for  $k = 1, 2, \dots, r$  do
6:       Compute feedback  $\beta_i^r(k)$  by Eq. (5).
7:        $F_i(r) = F_i(r) \cup \{\beta_i^r(k)\}$ 
8:     end for
9:     Compute  $\hat{d}_i(r)$  by Eq.(6).
10:  end for
11:  Find out estimated optimal action  $a_{m(r)}$  by Eq. (7).
12:  if  $r \geq R_s$  then
13:    for  $a_i \in A(r), i \neq m(r)$  do
14:      if  $|F_i(r)| \leq 30$  then
15:        Given  $F_{m(r)}(r), F_i(r)$  and  $\alpha$ , implement the t-test.
16:      else
17:        Given  $F_{m(r)}(r), F_i(r)$  and  $\alpha$ , implement the Z-test.
18:      end if
19:      if the null hypothesis  $H_0 : d_i = d_{m(r)}$  is rejected then
20:         $A(r+1) = A(r) \setminus \{a_i\}$ 
21:      end if
22:    end for
23:  end if
24:   $r = r + 1$ 
25: end while
26: return  $a_m(r), \hat{d}_m(r)$ 

```

3.2.1 Action set construction We construct the pool of prompts $L = \{\mathbf{p}_i\}_{i=1}^N$ with GPT-4 [1]. At the beginning, q prompts that have not been examined before are randomly chosen from L to form the action set A . The algorithm runs for multiple rounds and the action set at the r -th round is denoted by $A(r)$. Naturally, $|A(1)| = |A| = q$ and we set q to 5.

3.2.2 Feedback calculation At the r -th round, all the remaining actions in the action set $A(r)$ are chosen to interact with environment. To generate more feedback (thus reducing the bias in estimation the optimal prompt) with fewer queries, we conduct a cross-validation among all historical data. Concretely, for each action $a_i \in A(r)$, the feedback sequence $F_i(r)$ is appended with r extra feedback $F_i(r) = F_i(r-1) \cup \{\beta_i^r(k)\}_{k=1}^r$, where $\beta_i^r(k)$ is the relative KL divergence computed by Eq. (5), in which P, P', Q are estimated from nk images produced by f_0, f_0, f_m so far.

3.2.3 Action set updating strategy The action set updating strategy follows the statistical hypothesis testing proposed in Di et al. [8]. When the r -th round terminates, we compute the estimated reward probability $\hat{d}_i(r)$

$$\hat{d}_i(r) = \frac{\sum_{l=1}^r \sum_{k=1}^l \beta_i^l(k)}{|F_i(r)|}. \quad (6)$$

The estimated optimal action $a_{m(r)}$ after the r -th round is the one in $A(r)$ with the highest estimated reward probability $\hat{d}_i(r)$, i.e.:

$$a_{m(r)} = \arg \max_{a_i \in A(r)} \hat{d}_i(r). \quad (7)$$

After R_s rounds, the statistical hypothesis testing start. Following Di et al. [8], the Student’s t-test is adopted when $|F_i(r)| \leq 30$, while the Z-test is adopted in later rounds. For each non-optimal action $a_i \in A(r), i \neq m(r)$, the statistical test is conducted given the feedback sequences of action a_i and $a_{m(r)}$ and the significance level α . If the null hypothesis $H_0 : d_i = d_{m(r)}$ is rejected, action a_i is eliminated from the current action set. All the remaining actions in the action set are explored in later rounds

We remark that one difference between integrity verification and ordinary optimization is that it is sufficient to find one prompt that can distinguish two models (rather than find the most discriminating one). There is no need to run the algorithm until convergence as in the traditional LA. The entire process terminates after $\min(R, R_e)$ rounds and returns the most discriminating prompt at that time. The choice of R_e reflects a trade-off between algorithm performance and time consumption.

The overall process of the proposed PromptLA is summarized in Algorithm 1.

3.3 Integrity Verification Framework of T2I Diffusion Models

As shown in Figure 1, T2I diffusion models publisher can conduct the integrity verification when he/she suspects that a malicious user who has been authorized to use f_0 only for benign purposes modified the model for harmful purposes.

For a suspicious model f_m , the publisher first constructs a prompt library $L = \{\mathbf{p}_i\}_{i=1}^N$ and sets a threshold θ . Then PromptLA tests the prompt library gradually. Each time, the algorithm selects q prompts and returns the most discriminating prompt which is a_m from action set, and its corresponding relative KL divergence \hat{d}_m . If $\hat{d}_m \geq \theta$ then an integrity violation is reported. Otherwise, PromptLA continues to explore the remaining prompts in the library. If, after traversing the prompt library, no \hat{d}_m of prompts exceeds the set threshold θ , the model’s integrity is considered intact, and the highest value encountered during the process is recorded for the AUC calculation.

4 Experiments and Discussions

4.1 Settings

4.1.1 Original model to be protected We used Stable Diffusion (SD) [25] v1.5 as original model whose integrity needs to be protected. It is a fully open-source and widely adopted T2I diffusion model. In the experimental environment of this paper, using default parameters, it takes 5 seconds to access the SD-v1.5 and generate an image.

4.1.2 Integrity violations From the perspective of malicious users, the most commonly considered and the most easily applicable modifications are DreamBooth [26] and LoRA [27]. Other options include vanilla parameter modification or version rollback. They can hardly fulfill malicious purposes, but they serve as good examples

of integrity violations for evaluation. In summary, the integrity violations studied in this paper are:

- **DreamBooth¹**: **db1** to **db4** denotes four kinds of DreamBooth, each with different training data.
- **Stylized fine tuning**: **dl** denotes Dreamlike Diffusion 1.0, which is SD-v1.5 fine-tuned on high quality art.
- **Parameter modification**: **pa1** and **pa2**. Parameters of SD-v1.5 related to the attention mechanism (having the keyword "attentions" in their names) are added with various levels of random noise. The noise is uniformly sampled from the $[0, 1)$ interval and scaled by a coefficient that modulates its amplitude, with **pa1** set at 0.001 and **pa2** at 0.003.
- **Version rollback**: **v1.4** denotes using an older version model of stable diffusion, SD-v1.4.

4.1.3 Baselines For comparison, we transformed schemes designed for detection and tracing of generated images, such as **Color-based** [20], **Frequency-based** [10], and **Learning-based** [36] into baselines for integrity verification. Different from the original multi-classification task, baselines for integrity verification use some features of generated images as training samples to train a binary classifier under known attacks, which is then tested on a test set. We used CNN as the classifier after feature extraction for training. To make better comparisons, we trained the model using various training set compositions, such as single-violation generated images and a combination of multi-violation generated images, as shown in Table 3.

4.1.4 Metrics Integrity verification schemes are evaluated in their AUC in the binary classification between intact T2I models from modified ones. The cost of a scheme is measured in the number of images generated by the T2I diffusion models until the verification process terminates.

4.1.5 Implementation details In PromptLA, the number of images generated per prompt per model per round was set to $n = 5$, the starting round for filtering was $R_s = 5$, the total number of rounds was $R_e = 10$. We considered two configurations to the significance level α , and the threshold θ , as (0.01, 0.25) and (0.05, 0.3), which have good performance in comprehensive testing. These versions are denoted as **PromptLA_v1** and **PromptLA_v2**. All methods were repeated for 20 times for each different integrity violations to compute the AUC and the average cost.

4.2 Accuracy Evaluation

Table 3 shows that our method outperformed the baselines across various integrity violations, especially in detecting fine-grained modifications that are hard to spot. Although baselines achieved good detection results for known attacks such as db1 or db4 (i.e., the defender has known the modification that the adversary has performed), they performed poorly on unknown attacks, indicating a lack of generalization. Even if all potential violations are used to train the model, baselines exhibit good performance only on a small subset of them. In contrast, PromptLA selects the appropriate prompt for any integrity violation, which demonstrated strong performance and generalization capability. As shown in Figure 6, the

¹The dreambooth-lora method in Hugging Face with default configurations was used for training.

Table 3: Accuracy evaluation and comparison. Method¹ was trained on data generated from model after integrity violation db1, method² from db4, method³ from all 8 violations. The prompt chosen for baselines was prompt11 "Lion", which is more significant for most violations, as shown in Figure 3. Learning-based method also used Inception-v3 [31] model to extract features. The underscored portions indicate an AUC so low that it is effectively unusable. The 'avg' column represents the average AUC value across all 8 integrity violations for each method.

Method	Integrity Violation (AUC)								avg
	db1	db2	db3	db4	dl	pa1	pa2	v1.4	
Color-based [20] ¹	1.000	0.993	0.961	<u>0.286</u>	<u>0.028</u>	<u>0.284</u>	<u>0.561</u>	<u>0.161</u>	0.534
Color-based [20] ²	<u>0.000</u>	<u>0.000</u>	<u>0.526</u>	0.934	0.984	0.628	0.733	0.799	0.576
Color-based [20] ³	1.000	0.977	0.886	<u>0.523</u>	1.000	<u>0.046</u>	0.966	0.924	0.790
Frequency-based [10] ¹	1.000	<u>0.024</u>	<u>0.000</u>	<u>0.218</u>	<u>0.035</u>	<u>0.253</u>	<u>0.074</u>	<u>0.363</u>	0.246
Frequency-based [10] ²	<u>0.023</u>	0.984	0.991	0.617	0.986	0.705	0.987	<u>0.266</u>	0.695
Frequency-based [10] ³	<u>0.208</u>	0.958	0.926	0.835	1.000	<u>0.099</u>	0.969	<u>0.221</u>	0.652
Learning-based [36] ¹	1.000	1.000	0.998	<u>0.295</u>	<u>0.175</u>	<u>0.685</u>	<u>0.477</u>	<u>0.075</u>	0.588
Learning-based [36] ²	<u>0.169</u>	<u>0.288</u>	0.624	0.844	<u>0.556</u>	<u>0.090</u>	<u>0.344</u>	<u>0.108</u>	0.378
Learning-based [36] ³	1.000	1.000	1.000	0.591	0.998	<u>0.289</u>	0.934	<u>0.420</u>	0.779
PromptLA_v1 (Ours)	0.995	0.997	0.985	0.945	1.000	0.732	0.993	0.928	0.947
PromptLA_v2 (Ours)	1.000	1.000	0.997	0.995	1.000	0.690	0.997	0.953	0.954

prompt selected by **PromptLA_v2** exhibited higher discriminative qualities than random prompts.

If we remove the well-performing prompt11 "Lion" from the prompt library, which is shown in Figure 3, the performance of the baselines might be even worse. It is remarkable that they could still serve as promising integrity verification schemes against specific integrity violation, even though they were not designed for this purpose. However, due to the additional training costs involved, it is still less effective compared to the PromptLA algorithm.

4.3 Stability Evaluation

In practice, image-level post-processing operations such as cropping and compression might change the characteristics of images, leading to false integrity alarms. Therefore, an integrity verification algorithm should overlook such image-level post-processing. As shown in Figure 5, when being confronted by random cropping and 85% JPEG quality compression, **PromptLA_v1** and **PromptLA_v2** both maintained the high AUCs, indicating robust detection performance for various violations. For pa1 in **PromptLA_v2** against cropping and JPEG compression, the AUC even improved after image post-processing.

This demonstrates that the PromptLA algorithm's performance is stable under certain image-level post-processing such as random cropping and jpeg compression, thanks in part to the robustness of the image feature extraction model Inception-v3 [31].

4.4 Ablation Study

Finally, we evaluated the necessity of the PromptLA algorithm for integrity verification of T2I diffusion models through ablation studies. Without PromptLA, we employed a vanilla integrity verification framework where the prompt selection module Randomly picks and tests prompts from the library, using $n = 50$ images generated from the model for each prompt. **Random_v1** and **PromptLA_v1** used the same threshold $\theta = 0.25$, while **Random_v2** and **PromptLA_v2** used the same threshold $\theta = 0.3$.

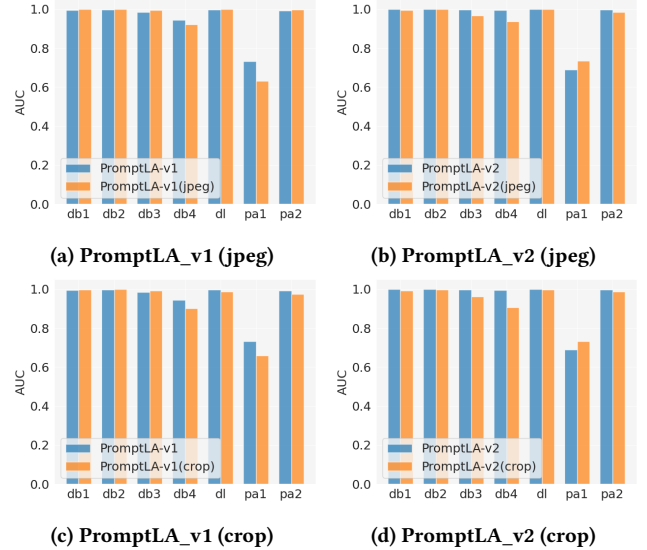


Figure 5: Stability evaluation against image-level post-processing such as random cropping and jpeg compression.

Table 4: Ablation study. Comparison of AUC and FPR with and without using the PromptLA algorithm. The 'FPR' column is the false positive rate when we use the original model as a violation to verify.

Method	FPR	Integrity Violation (AUC)			
	v1.5	db1	db4	pa1	v1.4
Random_v1	0.580	0.952	0.756	0.572	0.629
PromptLA_v1	0.100	0.995	0.945	0.732	0.928
Random_v2	0.350	0.982	0.886	0.654	0.768
PromptLA_v2	0.250	1.000	0.995	0.690	0.953

Table 5: Ablation study. Comparison of Cost with and without using the PromptLA algorithm. The value of Cost is the average number of images generated per detection.

Method	Integrity Violation (Cost)				
	v1.5	db1	db4	pa1	v1.4
Random_v1	1890	52	293	1159	1078
PromptLA_v1	1645	134	551	1354	846
Random_v2	2036	52	375	1709	1695
PromptLA_v2	1410	132	628	1375	859



Figure 6: A visual instance of prompt selection using the promptLA against integrity violation db1.

As shown in Table 4, without using PromptLA algorithm, for integrity violations that are difficult to detect such as db4, pa1, and SD-v1.4, the AUC decreased significantly, and the false positive rate (FPR) increased substantially, meaning a high likelihood of classifying an intact model as being modified. The reason is that without PromptLA, it is hard to accurately estimate the distribution of generated images, so the verification is corrupted by the high bias.

As shown in Table 5, for easier integrity violations, random strategies has a lower cost, as most prompts can provide sufficient discrimination. On the other hand, PromptLA has better efficiency for more challenging integrity violations that are harder to identify. Because PromptLA can quickly eliminate less effective prompts at a minimal cost, thus reaching a balance between accuracy and efficiency.

4.5 Discussion

The magnitude of integrity violations partially determines the difficulty of spotting them. However, different types of integrity violations can hardly be measured with respect to a unified metric regarding magnitude, either the distance in parameters or that in decision boundaries does not turn out to be conclusive. Due to a consistency concern, we studied this effect by confining the category of modifications to parameter-level modifications, where there is a well-defined order among all modification. As shown in Table 6, when the degree of T2I diffusion model parameter modification gradually increased, so did the AUC of integrity verification. Meanwhile, the Cost decreased for both **PromptLA_v1** and **PromptLA_v2**, which result indicated that integrity violations of a larger magnitude are easier to detect. However, a theoretically unified and convincing metric on the magnitude of integrity violations to deep neural networks, including T2I models, remains a challenge to be addressed.

Table 6: Integrity verification results vary when parameters are added with various levels of random noise. The noise was uniformly sampled from [0, 1) and scaled by a coefficient that modulates its amplitude. The amplitude coefficient ranged from 0.0010 to 0.0035, with the parameter differences between models measured using Euclidean distance.

Amplitude Coefficient	Euclidean Distance	PromptLA_v1		PromptLA_v2	
		AUC	Cost	AUC	Cost
0.0010	110.19	0.732	1354	0.690	1375
0.0015	165.24	0.865	1221	0.720	1465
0.0020	220.31	0.933	533	0.920	746
0.0025	275.37	0.950	303	0.975	349
0.0030	330.48	0.993	148	0.997	148
0.0035	385.51	1.000	126	1.000	127

5 Conclusion

In this paper, we propose an integrity verification scheme of T2I diffusion models. Considering the randomness, complexity, and high querying cost associated with T2I diffusion models, we measure the modifications to the underlying model through the differences in the feature distributions of generated images, and propose a prompt selection algorithm based on learning automaton (PromptLA). Extensive experimental results demonstrate that our algorithm offers superior detection accuracy, efficiency, and generalization. PromptLA’s performance remains stable under image-level post-processing. The discussion in the experimental section regarding the impact of the degree of integrity tampering on detection results is currently limited to parameter modifications, yet it paves the way to more comprehensive metrics to measure the level of integrity violations. In our future work, we will explore optimizing prompts in continuous spaces and aim to extend the integrity verification framework to various complex generative tasks beyond text-to-image.

References

- [1] Josh Achiam, Steven Adler, Sandhini Agarwal, Lama Ahmad, Ilge Akkaya, Florencia Leoni Aleman, Diogo Almeida, Janko Altenschmidt, Sam Altman, Shyamal Anadkat, et al. 2023. Gpt-4 technical report. *arXiv preprint arXiv:2303.08774* (2023).
- [2] Omid Aramoon, Pin-Yu Chen, and Gang Qu. 2021. Aid: Attesting the integrity of deep neural networks. In *2021 58th ACM/IEEE Design Automation Conference (DAC)*. IEEE, 19–24.
- [3] Negin Ayoughi, Shiva Nejati, Mehrdad Sabetzadeh, and Patricio Saavedra. 2024. Enhancing Automata Learning with Statistical Machine Learning: A Network Security Case Study. *arXiv preprint arXiv:2405.11141* (2024).
- [4] Eva Cetinic, Tomislav Lipic, and Sonja Grgic. 2018. Fine-tuning convolutional neural networks for fine art classification. *Expert Systems with Applications* 114 (2018), 107–118.
- [5] Anuran Chakraborty, Kushal Kanti Ghosh, Rajonya De, Erik Cuevas, and Ram Sarkar. 2021. Learning automata based particle swarm optimization for solving class imbalance problem. *Applied Soft Computing* 113 (2021), 107959.
- [6] Jia Deng, Wei Dong, Richard Socher, Li-Jia Li, Kai Li, and Li Fei-Fei. 2009. Imagenet: A large-scale hierarchical image database. In *2009 IEEE conference on computer vision and pattern recognition*. Ieee, 248–255.
- [7] Chong Di, Fangqi Li, Pengyao Xu, Ying Guo, Chao Chen, and Minglei Shu. 2023. Learning automata-accelerated greedy algorithms for stochastic submodular maximization. *Knowledge-Based Systems* 282 (2023), 111118.
- [8] Chong Di, Shenghong Li, Fangqi Li, and Kaiyue Qi. 2019. A novel framework for learning automata: a statistical hypothesis testing approach. *IEEE Access* 7 (2019), 27911–27922.

- [9] Ming Ding, Zhuoyi Yang, Wenyi Hong, Wendi Zheng, Chang Zhou, Da Yin, Junyang Lin, Xu Zou, Zhou Shao, Hongxia Yang, et al. 2021. Cogview: Mastering text-to-image generation via transformers. *Advances in neural information processing systems* 34 (2021), 19822–19835.
- [10] Ricard Durall, Margret Keuper, and Janis Keuper. 2020. Watch your up-convolution: Cnn based generative deep neural networks are failing to reproduce spectral distributions. In *Proceedings of the IEEE/CVF conference on computer vision and pattern recognition*. 7890–7899.
- [11] Pierre Fernandez, Guillaume Couairon, Hervé Jégou, Matthijs Douze, and Teddy Furon. 2023. The stable signature: Rooting watermarks in latent diffusion models. In *Proceedings of the IEEE/CVF International Conference on Computer Vision*. 22466–22477.
- [12] Rinon Gal, Yuval Alaluf, Yuval Atzmon, Or Patashnik, Amit H Bermano, Gal Chechik, and Daniel Cohen-Or. 2022. An image is worth one word: Personalizing text-to-image generation using textual inversion. *arXiv preprint arXiv:2208.01618* (2022).
- [13] Ian Goodfellow, Jean Pouget-Abadie, Mehdi Mirza, Bing Xu, David Warde-Farley, Sherjil Ozair, Aaron Courville, and Yoshua Bengio. 2014. Generative adversarial nets. *Advances in neural information processing systems* 27 (2014).
- [14] Ian Goodfellow, Jean Pouget-Abadie, Mehdi Mirza, Bing Xu, David Warde-Farley, Sherjil Ozair, Aaron Courville, and Yoshua Bengio. 2020. Generative adversarial networks. *Commun. ACM* 63, 11 (2020), 139–144.
- [15] Zecheng He, Tianwei Zhang, and Ruby Lee. 2019. Sensitive-sample fingerprinting of deep neural networks. In *Proceedings of the IEEE/CVF conference on computer vision and pattern recognition*. 4729–4737.
- [16] John R Hershey and Peder A Olsen. 2007. Approximating the Kullback Leibler divergence between Gaussian mixture models. In *2007 IEEE International Conference on Acoustics, Speech and Signal Processing-ICASSP'07*, Vol. 4. IEEE, IV–317.
- [17] Jonathan Ho, Ajay Jain, and Pieter Abbeel. 2020. Denoising diffusion probabilistic models. *Advances in neural information processing systems* 33 (2020), 6840–6851.
- [18] Diederik P Kingma and Max Welling. 2013. Auto-encoding variational bayes. *arXiv preprint arXiv:1312.6114* (2013).
- [19] Fang-Qi Li, Shi-Lin Wang, and Alan Wee-Chung Liew. 2023. Linear Functionality Equivalence Attack Against Deep Neural Network Watermarks and a Defense Method by Neuron Mapping. *IEEE Transactions on Information Forensics and Security* 18 (2023), 1963–1977.
- [20] Scott McCloskey and Michael Albright. 2018. Detecting gan-generated imagery using color cues. *arXiv preprint arXiv:1812.08247* (2018).
- [21] Kumpati S Narendra and Mandayam AL Thathachar. 2012. *Learning automata: an introduction*. Courier corporation.
- [22] Alex Nichol, Prafulla Dhariwal, Aditya Ramesh, Pranav Shyam, Pamela Mishkin, Bob McGrew, Ilya Sutskever, and Mark Chen. 2021. Glide: Towards photorealistic image generation and editing with text-guided diffusion models. *arXiv preprint arXiv:2112.10741* (2021).
- [23] Aditya Ramesh, Prafulla Dhariwal, Alex Nichol, Casey Chu, and Mark Chen. 2022. Hierarchical text-conditional image generation with clip latents. *arXiv preprint arXiv:2204.06125* 1, 2 (2022), 3.
- [24] Aditya Ramesh, Mikhail Pavlov, Gabriel Goh, Scott Gray, Chelsea Voss, Alec Radford, Mark Chen, and Ilya Sutskever. 2021. Zero-shot text-to-image generation. In *International conference on machine learning*. Pmlr, 8821–8831.
- [25] Robin Rombach, Andreas Blattmann, Dominik Lorenz, Patrick Esser, and Björn Ommer. 2022. High-resolution image synthesis with latent diffusion models. In *Proceedings of the IEEE/CVF conference on computer vision and pattern recognition*. 10684–10695.
- [26] Nataniel Ruiz, Yuanzhen Li, Varun Jampani, Yael Pritch, Michael Rubinstein, and Kfir Aberman. 2023. Dreambooth: Fine tuning text-to-image diffusion models for subject-driven generation. In *Proceedings of the IEEE/CVF conference on computer vision and pattern recognition*. 22500–22510.
- [27] Simo Ryu. 2023. Low-rank adaptation for fast text-to-image diffusion fine-tuning. *Low-rank adaptation for fast text-to-image diffusion fine-tuning* (2023).
- [28] Chitwan Saharia, William Chan, Saurabh Saxena, Lala Li, Jay Whang, Emily L Denton, Kamyar Ghasemipour, Raphael Gontijo Lopes, Burcu Karagol Ayan, Tim Salimans, et al. 2022. Photorealistic text-to-image diffusion models with deep language understanding. *Advances in neural information processing systems* 35 (2022), 36479–36494.
- [29] Mohammad Savargiv, Behrooz Masoumi, and Mohammad Reza Keyvanpour. 2022. A new ensemble learning method based on learning automata. *Journal of Ambient Intelligence and Humanized Computing* 13, 7 (2022), 3467–3482.
- [30] Hae Jin Song, Mahyar Khayatkhoei, and Wael AbdAlmageed. 2024. ManiFPT: Defining and Analyzing Fingerprints of Generative Models. In *Proceedings of the IEEE/CVF Conference on Computer Vision and Pattern Recognition*. 10791–10801.
- [31] Christian Szegedy, Vincent Vanhoucke, Sergey Ioffe, Jon Shlens, and Zbigniew Wojna. 2016. Rethinking the inception architecture for computer vision. In *Proceedings of the IEEE conference on computer vision and pattern recognition*. 2818–2826.
- [32] Shuo Wang, Sharif Abuadba, Sidharth Agarwal, Kristen Moore, Ruoxi Sun, Minhui Xue, Surya Nepal, Seyit Camtepe, and Salil Kanhere. 2023. Publiccheck: Public integrity verification for services of run-time deep models. In *2023 IEEE Symposium on Security and Privacy (SP)*. IEEE, 1348–1365.
- [33] Yuxin Wen, John Kirchenbauer, Jonas Geiping, and Tom Goldstein. 2023. Treeing watermarks: Fingerprints for diffusion images that are invisible and robust. *arXiv preprint arXiv:2305.20030* (2023).
- [34] Dongxian Wu and Yisen Wang. 2021. Adversarial neuron pruning purifies backdoored deep models. *Advances in Neural Information Processing Systems* 34 (2021), 16913–16925.
- [35] Zhaoxia Yin, Heng Yin, Hang Su, Xinpeng Zhang, and Zhenzhe Gao. 2023. Decision-based iterative fragile watermarking for model integrity verification. *arXiv preprint arXiv:2305.09684* (2023).
- [36] Ning Yu, Larry S Davis, and Mario Fritz. 2019. Attributing fake images to gans: Learning and analyzing gan fingerprints. In *Proceedings of the IEEE/CVF international conference on computer vision*. 7556–7566.
- [37] Rizgar Zebari, Adnan Abdulazeez, Diyar Zeebaree, Dilovan Zebari, and Jwan Saeed. 2020. A comprehensive review of dimensionality reduction techniques for feature selection and feature extraction. *Journal of Applied Science and Technology Trends* 1, 1 (2020), 56–70.
- [38] Hongyu Zhu, Sichu Liang, Wentao Hu, Li Fangqi, Ju Jia, and Shi-Lin Wang. 2024. Reliable Model Watermarking: Defending Against Theft without Compromising on Evasion. In *Proceedings of the 32nd ACM International Conference on Multimedia*. 10124–10133.
- [39] Zhiying Zhu, Hang Zhou, Siyuan Xing, Zhenxing Qian, Sheng Li, and Xinpeng Zhang. 2022. Perceptual hash of neural networks. *Symmetry* 14, 4 (2022), 810.
- [40] Michael J Zyphur and Frederick L Oswald. 2015. Bayesian estimation and inference: A user's guide. *Journal of Management* 41, 2 (2015), 390–420.